

See discussions, stats, and author profiles for this publication at: <https://www.researchgate.net/publication/228482224>

Simultaneous Synthesis of Polyaniline Nanotubules and Gold Nanoplates

ARTICLE in CRYSTAL GROWTH & DESIGN · MAY 2008

Impact Factor: 4.89 · DOI: 10.1021/cg060895c

CITATIONS

12

READS

28

8 AUTHORS, INCLUDING:



Junhua Yuan

Zhejiang Normal University

35 PUBLICATIONS 626 CITATIONS

SEE PROFILE



Yuanjian Zhang

Southeast University (China)

81 PUBLICATIONS 3,130 CITATIONS

SEE PROFILE



Li Niu

Chinese Academy of Sciences

215 PUBLICATIONS 7,050 CITATIONS

SEE PROFILE



Ari Ivaska

Åbo Akademi University

319 PUBLICATIONS 9,588 CITATIONS

SEE PROFILE

Simultaneous Synthesis of Polyaniline Nanotubules and Gold Nanoplates

Zhijuan Wang,^{†,*} Junhua Yuan,[†] Dongxue Han,[†] Yuanjian Zhang,[†] Yanfei Shen,[†]
Daniel Kuehner,[†] Li Niu,^{*,†,*} and Ari Ivaska[‡]

State Key Laboratory of Electroanalytical Chemistry, Changchun Institute of Applied Chemistry,
Graduate School of the Chinese Academy of Sciences, Chinese Academy of Sciences,
Changchun 130022, P. R. China, and Laboratory of Analytical Chemistry, Process Chemistry Centre,
Åbo Akademi University, Biskopsgatan 8, FI-20500 Åbo-Turku, Finland

Received December 7, 2006; Revised Manuscript Received February 7, 2008

ABSTRACT: This paper describes a facile route for simultaneous synthesis of polyaniline (PANI) nanotubules and gold nanoplates. The inner diameter of PANI nanotubules was less than 10 nm and the length was several micrometers. At the same time, uniform single-crystal gold nanoplates with thicknesses of tens of nanometers were obtained. The resulting products are characterized further by scanning electron microscopy (SEM), transmission electron microscopy (TEM), and FT-IR spectroscopy. The effect of concentration ratios of the HAuCl_4 to aniline to this synthesis is also studied.

1. Introduction

Among conducting polymers, polyaniline (PANI) has been extensively studied because of its easy polymerization, chemical stability, relatively high conductivity, and potential applications in electronic devices, batteries, and sensors.¹ Many of those applications depend on generating one-dimensional (1D) nanostructures.² Recently, PANI nanowires, rods, tubes, and fibers have been studied with the expectation that such materials will possess the advantages of both low-dimensional systems and organic conductors.^{3–5} Among these nanostructures, hollow nanotubules have attracted increasing attention, mainly for potential application in catalysis, drug delivery, microelectronics, energy storage/conversion, and design of biomimetic membranes and channels.^{6–9} Despite being more difficult to fabricate than nanospheres, rods or fibers, PANI micro- and nanotubules have been successfully synthesized by several groups.^{10–12} In particular, various template-assisted approaches have been reported in preparing monodispersed PANI micro- and nanotubes with controllable diameter, length, and conductivity. However, tedious postprocessing is required to remove the hard template.¹³ Removal of the template often affects the structure of the material, especially the hollow polymer microstructures.¹⁴

Comparing with the hard template-assisted method, the soft-template method is very useful in preparing conducting polymers nanotubes in large amount because it does not need any complicated post-treatment procedures after polymerization. Nanostructured PANI has been synthesized by using a variety of oxidants, including ammonium peroxydisulfate,^{11,13} sodium vanadates,¹² and hydrogen peroxide.¹⁵ Additional methods using metallic-anion oxidants have also been reported. For example, Möller et al. reported formation of gold-polypyrrole core-shell particles using tetrachloroaurate (AuCl_4^-),¹⁶ whereas Sastry et al. demonstrated oxidative polymerization of diamine by tetrachloroaurate ions.¹⁷ Similarly, Liu prepared polypyrrole-stabilized gold nanostructures by polymerization of pyrrole in the presence of gold ions over roughened gold substrates.¹⁸ Several authors have also applied tetrachloroaurate in oxidative polymerization of aniline, obtaining gold nanostructures and

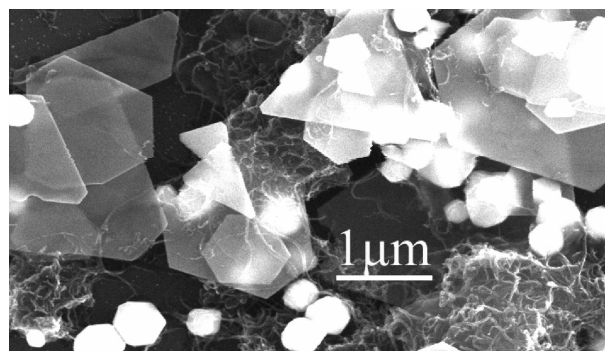


Figure 1. SEM image of precipitated product prepared by combining 0.48 mL of aniline, 4.00 mL of HAc, 0.25 g of CTAB, and 0.007 g of $\text{HAuCl}_4 \cdot 3\text{H}_2\text{O}$.

PANI-Au composites.^{19–23} However, in those works, the emphasis was on preparing composite materials, and the morphology of obtained PANI powder showed mainly short solid/hollow nanorods including some nonfibrous particulates.^{24–26} Anisotropic growth (one-dimensional (1D) elongation) is suppressed in such a system. In the work, PANI nanotubules (with inner diameters of <10 nm and lengths of several micrometers) and gold nanostructures were prepared via a similar soft-template method. Upon aniline/HAc/Cetyltrimethylammonium bromide (CTAB) and HAuCl_4 solutions being mixed at room temperature, PANI nanotubules and gold nanoplates are simultaneously formed. Formation of PANI and gold nanostructures resulted from two kinds of soft templates, which is different from the traditional soft-template method. Comparing with previous reports²⁷ our method is an easy and effective way to prepare PANI nanotubules with small diameter (<10 nm) and long tubes. In addition, the synthesized PANI nanotubules and gold nanoplates are separate entities without any interaction.

2. Materials and Methods

2.1. Materials. CTAB (99.0%), acetic acid (HAc, 99.5%), and methanol (99.5%) were obtained from Beijing Chemical Factory and used without any further purification. Chloroauric acid hydrate ($\text{HAuCl}_4 \cdot 3\text{H}_2\text{O}$, 99.999%) was obtained from Aldrich and used as received. Aniline (99.5%, Beijing Chemical

* Corresponding author. Fax: 86-431-8526 2800. E-mail: lniu@ciac.jl.cn.

[†] Chinese Academy of Sciences.

[‡] Åbo Akademi University.

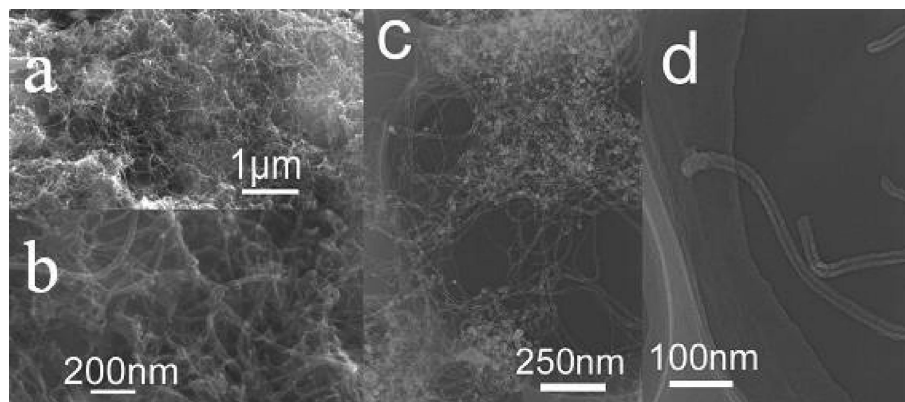


Figure 2. SEM images of nanotubes at (a) low magnification and (b) high magnification; TEM images of nanotubes at (c) low magnification and (d) high magnification.

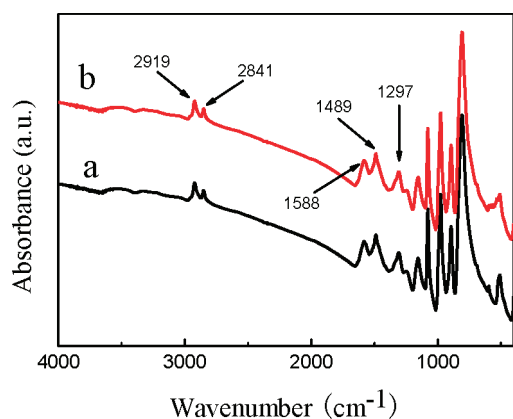


Figure 3. FTIR spectra of (a) methanol-extracted PANI nanotubes and (b) crude product.

Factory) was distilled under nitrogen at reduced pressure, and then stored below 0 °C. All aqueous solutions were prepared with ultrapure water (>18 MΩ cm) obtained from a Milli-Q Plus system (Millipore). All experiments were carried out at room temperature.

2.2. Synthesis of PANI Nanotubes and Gold Nanoplates.

In a standard synthesis, 0.48 mL of distilled aniline was added dropwise to a 0.17 M solution of CTAB in glacial acetic acid (0.25 g CTAB in 4.00 mL) under vigorous agitation. After mixing for several minutes, 1.00 mL of 17.8 mM aqueous $\text{HAuCl}_4 \cdot 3\text{H}_2\text{O}$ (0.007 g) was added dropwise under continued agitation. In the final solution, the concentrations of aniline, CTAB, and HAuCl_4 were 96, 125, and 3, respectively, with aniline-to-gold molar ratio 296:1. The color of the solution changed immediately from straw yellow to orange and then to deep red as gold nanostructures formed. The solution was then stirred for an additional 8 h and the color changed to green, indicative of PANI. Centrifugation yielded a gold-colored precipitate, which was washed several times with Milli-Q water by successive resuspension and centrifugation, then dried under a vacuum at 60 °C overnight.

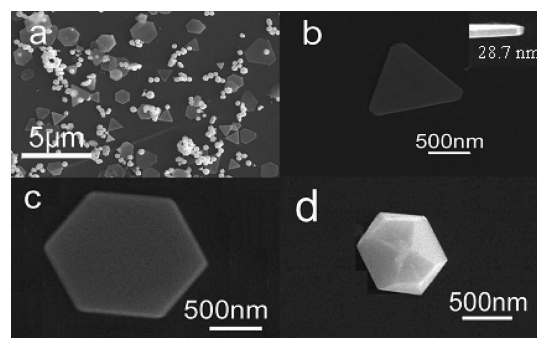
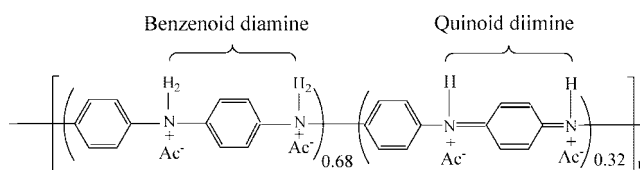


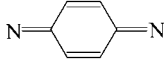
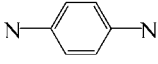
Figure 4. SEM images of gold nanomaterials obtained after methanol extraction of crude product: (a) low magnification, (b–d) higher magnifications.

Scheme 1. Molecular Structure of PANI Doped with Acetic Acid



2.3. Characterization. Product morphology was examined by transmission electron microscopy, using a JEOL 2010 TEM at 200 kV, and by scanning electron microscopy, using an XL30 ESEM FEG with accelerating voltage 20 kV. Samples for SEM and TEM measurements were prepared by dispersing the precipitate in ethanol and casting several drops of the dispersion onto a silicon wafer, then evaporating in ambient air. Because of the good electrical conductivity of the precipitate, sputter-coating of a conductive thin layer was not necessary. X-ray diffraction (XRD) patterns were collected using a D/Max 2500 V/PC X-ray diffractometer with high-intensity $\text{Cu K}\alpha$ (40 kV, 200 mA) radiation. FTIR spectra were obtained using a Bruker Tensor 27 Spectrometer with samples in KBr pellet form.

Table 1. FTIR Band Assignments for PANI Doped with Acetic Acid

C-H out-of-plane bending	 quinoid deformation	C-N stretching	C=N stretching	 benzenoid deformation (emeraldine)
807 cm^{-1}	1582 cm^{-1}	1307 cm^{-1}	1237 cm^{-1}	1487 cm^{-1}

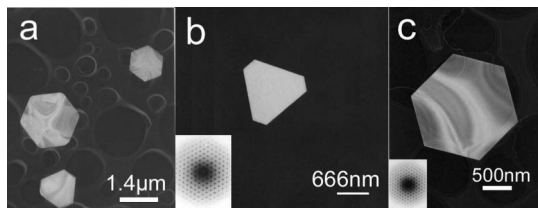


Figure 5. TEM images of gold nanomaterials obtained after methanol extraction of crude product and corresponding electron diffraction patterns.

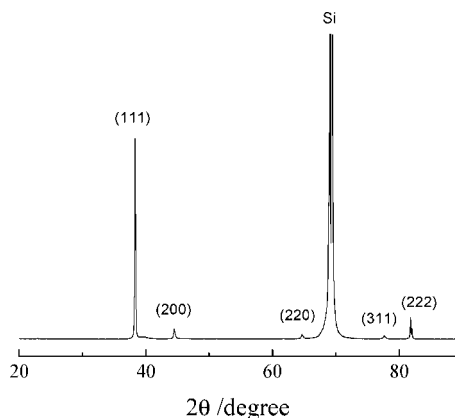


Figure 6. Representative XRD pattern of precipitated gold nanomaterials.

UV–visible absorbance spectra were acquired using a Cary 500 UV–vis NIR spectrometer (Varian).

3. Results and Discussion

Figure 1 is a SEM image of a typical crude precipitated product. Triangular and polygonal gold nanoplates are mixed with smaller, brighter gold crystallites, together with a highly entangled network structure. When the crude product was

suspended in methanol, a clear green upper liquid phase was formed, indicating that the dissolved phase contained oligomer. The precipitate phase left was yellow, obviously containing the gold materials. The entire crude product was suspended also in ethanol and samples for the SEM and TEM measurements were done as described in the chapter 2.3. The SEM and TEM images are shown in Figure 2, where flexible entangled nanofibers with length up to several micrometers can be seen. At higher magnification (Figure 2d) the fibers are clearly seen to be hollow nanotubules with an average inner diameter of ca. 8 nm, as measured by the TEM image-analysis software.

Samples of the methanol phase and the solid crude product pressed in a KBr pellet were examined by FTIR spectroscopy and the spectra are shown in Figure 3. Presence of PANI is confirmed by the characteristic peaks in the range 700–1600 cm^{-1} , with band assignments given in Table 1. The bands for the benzenoid and quinoid groups are particularly important because they show the oxidation state of the polymer.²⁸ The broad band in the region of 4000–2000 cm^{-1} is due to the free carriers.

Because there are no shifts between the peaks in the spectrum of extracted PANI (Figure 3a) and PANI in the crude product (Figure 3, curve b), there is not any interaction between gold and PANI in the crude product. Additionally, the oxidation state of PANI can be estimated from the ratio of integrated peak areas for quinoid (1582 cm^{-1}) and benzenoid (1487 cm^{-1}) phenyl rings, as illustrated in Scheme 1, showing the oxidized structure of PANI doped with acetic acid.¹⁹ The ratio (i.e., oxidation state to reduction state) across several samples was 0.46 ± 0.02 , indicating the reduced benzenoid state was dominant (Scheme 1).

Figure 4 shows SEM images of the yellow precipitated material obtained after methanol extraction of the crude product. Images b and c in Figure 4 show the truncated triangular and micrometer-scale hexagonal plates at greater magnification. The inset in Figure 4b shows an edge-on view of a representative plate with the estimated thickness (28.7 nm) determined by the SEM image-analysis software. Figure 4d is magnification of a

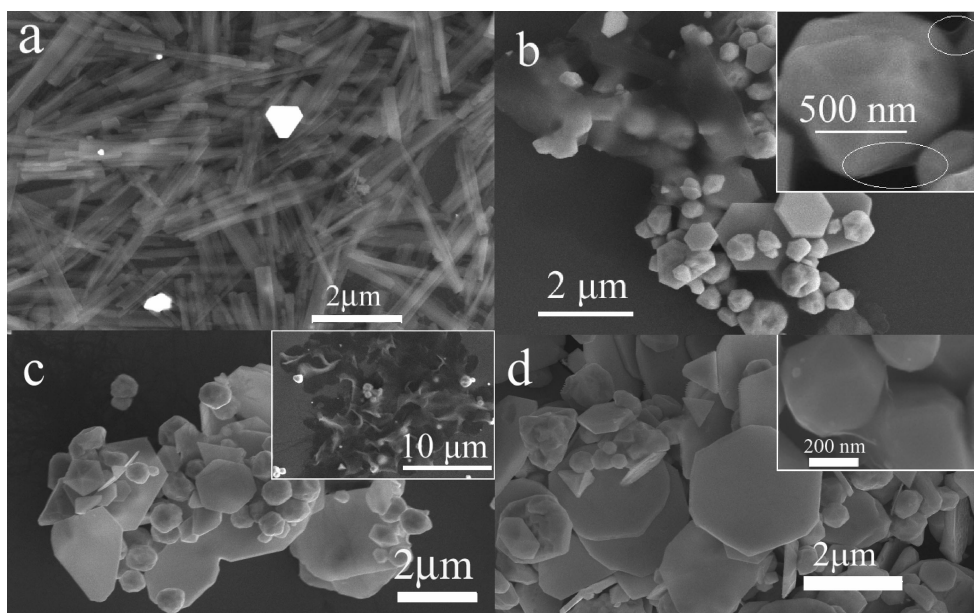


Figure 7. SEM images of typical products obtained with the following aniline-to- HAuCl_4 molar ratios: (a) 750:1, (b) 500:1, (c) 125:1, and (d) 83:1. In all reactions, the volume of HAc (4.00 mL) and the amount of CTAB (0.25 g) were constant. Ovals in the inset of image b highlight PANI wrapped around gold polyhedra.

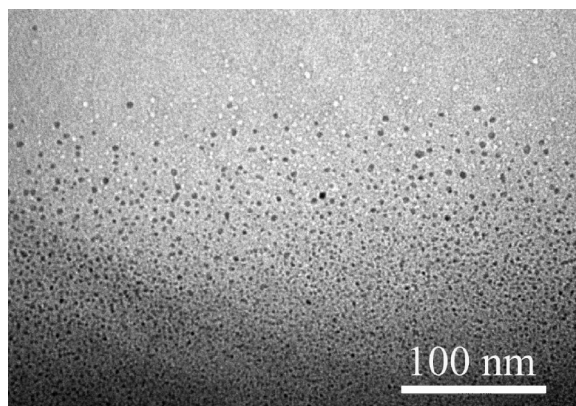


Figure 8. TEM image of micelles formed in a reaction mixture containing 0.48 mL of aniline, 4.00 mL of HAC, and 0.25 g of CTAB.

representative small white particle from Figure 4a, showing a polyhedral structure.

Images b and c in Figure 5 are TEM images of triangular and hexagonal gold nanoplates. The insets show the corresponding area-selected electron diffraction patterns, confirming the nanoplates to be single crystals bounded mainly by (111) facets.²⁹ The bandlike patterns shown on the surface of the nanoplate in Figure 5c are ascribed to differences in electron density.²⁹ Similar bandlike patterns have also been reported by other research groups in their nanoplates.^{29–31}

Examination of the crude product with XRD gave the pattern shown in Figure 6, which clearly indicates the presence of fcc gold. The (200):(111) and (220):(111) peak intensity ratios are much lower than the accepted reference values³¹ (0.05 versus 0.53 and 0.024 versus 0.33, respectively), indicating that the gold nanomaterials are dominated by (111) facets oriented parallel to the supporting substrate surface.

To determine the effect of relative concentrations of aniline and HAuCl_4 on product morphology, we varied the [aniline]: $[\text{HAuCl}_4]$ molar ratio roughly 10-fold across a series of reactions. SEM images of typical products are shown in Figure 7. At the highest aniline-to-gold ratio (Figure 7a), PANI rods were the primary product, with only a few gold plates. With increasing relative amount of HAuCl_4 , polygonal plates and then polyhedral particles became the dominant gold products (Figure 7b–d), and PANI films were observed either wrapped around gold polyhedra (insets to b and d in Figure 7) or as isolated films (Figure 7c, inset).

In all reactions reported here, the CTAB concentration was 2 orders of magnitude higher than the critical micelle concentration (cmc , about 8×10^{-4} M at room temperature³²). The TEM image (Figure 8) confirmed the presence of globular micelles of 3–5 nm diameters after addition of aniline to the CTAB/acetic acid solution. In a control experiment, however, where distilled water was used as solvent instead of acetic acid as solvent, no micelles were observed, indicating that acetic acid is necessary for the micelle formation. But the precise role of micelles in these reaction systems is still under investigation.

To clarify the role of HAC in the reaction mechanism, we performed control experiments. In these experiments, 0.25 g of CTAB was added to 4.00 mL of distilled water, and glacial HAC resulting mixtures are shown in Figure 9a. Homogeneous, colored solutions were obtained when glacial HAC was used as solvent (vial B). However, the mixture split into two liquid phases when CTAB was added to pure water (vial A). Subsequently, 0.48 mL of aniline was added to each of the vials

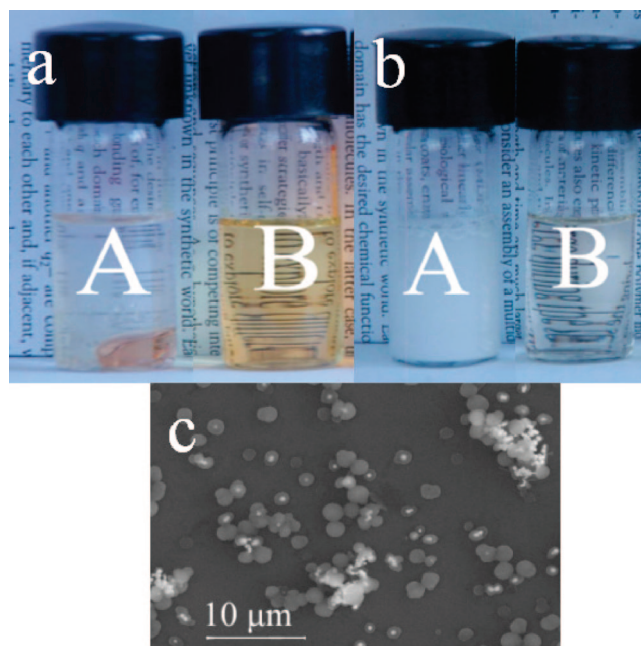


Figure 9. (a) Mixtures obtained from adding 0.25 g of CTAB to (A) 4.00 mL of H_2O and (B) 4.00 mL of HAC, and (b) after adding 0.48 mL of aniline to each mixture. (c) SEM image of crude products obtained after the addition of 0.007 g of $\text{HAuCl}_4 \cdot 3\text{H}_2\text{O}$ in 1.00 mL of water to vial A shown in b.

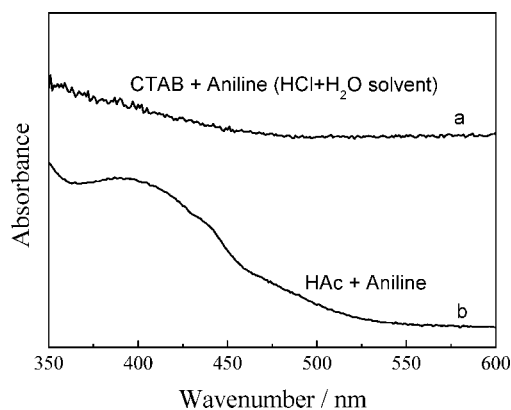
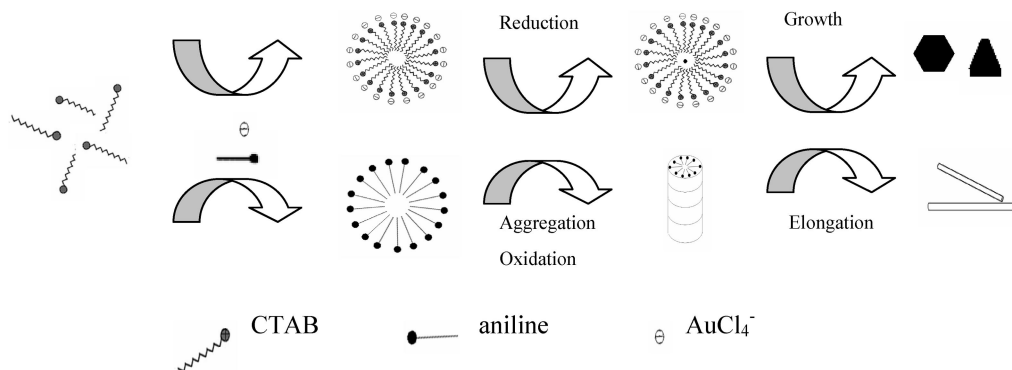


Figure 10. UV-vis spectra of mixtures containing (a) 0.48 mL of aniline, 2.00 mL of HCl, 2.00 mL of H_2O , and 0.25 g of CTAB; (b) 0.48 mL of aniline and 4.00 mL of HAC.

and mixed thoroughly, to give the mixtures shown in Figure 9b. Although the glacial HAC-containing solutions remained homogeneous and became largely colorless (vial B), a milky white suspension formed in vial A. These observations indicate that acetic acid is a better solvent than water for both CTAB and aniline. The clear solution in vial B in Figure 9b indicated that aniline might react with acetic acid to form $\text{PhNH}_3^+\text{Ac}^-$. The reaction between aniline and acetic acid was confirmed by UV-vis spectroscopy (Figure 10). The broad peak approximately at 400 nm (curve b) indicates that aniline monomer reacted with HAC, not with CTAB.

Subsequently, 0.007 g of $\text{HAuCl}_4 \cdot 3\text{H}_2\text{O}$ in 1.00 mL of water was added to vial A (Figure 9b), and the reaction was allowed to equilibrate at room temperature for 8 h. SEM image of the crude products is shown in Figure 9c. In distilled water, small gold particles wrapped with PANI films were formed. PANI nanotubules, however, were not formed in this reaction.

Scheme 2. Schematic Depiction of Different Periods during the Formation of the PANI Nanotubes and Gold Nanoplates



On the basis of the results of the experiments, a mechanism for the formation of PANI nanotubes and gold nanoplates was proposed (Scheme 2). In HAC-aniline-CTAB mixtures, anilinium acetate salts may form. According to the results of UV-vis measurements, the salt was formed as $\text{PhNH}_3^+\text{Ac}^-$. The anilinium cations can form micelles and might act as the templates to form PANI nanotubes.³³ After addition of the aqueous chloroaurate solution, AuCl_4^- associates strongly with the positively charged CTAB micelles.³⁴ Because the products of PANI and gold nanomaterials did not interact with each other, these two kinds of micelles should be formed separately. On the basis of these considerations, in the experiment, anilinium cations micelles and CTAB-tetrachloroaurate micelles form in the solution, respectively. And the reduction of HAuCl_4 and oxidation of aniline occur simultaneously, leading to the formation of small gold nanoparticles and aniline oligomers, respectively. Once reduced, the small gold nanoparticles are protected from aggregation by the CTAB micelles before the formation of other kind of gold nanostructures. Because the (111) face of fcc packing has the lowest sticking probability due to the lowest surface energy compared to other faces ($\gamma(110) > \gamma(100) > \gamma(111)$), the fcc facet confers its tendency to nucleate and grow into nanoparticles with their surfaces bounded by (111) facets.³⁵ Accordingly, the selective interaction between CTAB and Au nanocrystals could greatly reduce the growth rate along the (111) direction and enhance the growth rate along the (110) direction, which can facilitate the formation of the platelike or other anisotropic Au nanostructures. Aniline polymerization takes place mainly in the micelle-water interface adjacent to the CTAB headgroups because the oxidant, AuCl_4^- anions were attached to CTAB micelles. Subsequently, the micelles may become tubes and PANI nanotubes was finally formed via a possible self-assembly process. The weak oxidant (AuCl_4^-) made the growing process slow and formed uniform nanotubes comparing with the previous report.²⁷

4. Conclusion

PANI and gold nanoplates have been prepared simultaneously by mixing aniline acidified with glacial acetic acid and chloroauric acid hydrate in the presence of CTAB at room temperature. The aniline monomer is oxidized into PANI with corresponding reduction of chloroaurate to fcc gold nanoplates and gold polyhedra. In certain reaction conditions, the PANI is obtained as nanotubes with inner diameters less than 10 nm and lengths of several micrometers, and gold nanoplates are large, uniform, single crystals with thicknesses of about a few tens of nanometers. The UV-vis results indicate that aniline monomer does not react with CTAB, but with glacial HAC. On the basis of these results, it is proposed that CTAB and anilinium salt micelles form during the synthesis. Formation of single

crystal fcc gold nanoplates is due to selective growth of (111) side planes, whereas PANI nanotubes may be synthesized via a self-assembly process. In further studies, the electrical conductivity of an individual PANI nanotube can be measured whereas the gold nanoplates and polyhedra might be used as substrates for the surface-enhanced Raman scattering (SERS) measurements.

Acknowledgment. The authors are most grateful to the NSFC, China (20475053 and 20673109) and to the Department of Science and Technology of Jilin Province (20050102) for the financial support.

References

- (1) Mallick, K.; Witcomb, M. J.; Dinsmore, A.; Scurrall, M. S. *Macromol. Rapid Commun.* **2005**, *26*, 232.
- (2) Zhang, X. T.; Zhang, J.; Liu, Z. F.; Robinson, C. *Chem. Commun.* **2004**, *16*, 1852.
- (3) Ma, Y. F.; Zhang, J. M.; Zhang, G. J.; He, H. X. *J. Am. Chem. Soc.* **2004**, *126*, 7097.
- (4) Xia, H. B.; Narayanan, J.; Cheng, D. M.; Xiao, C. Y.; Liu, X. Y.; Chan, H. S. O. *J. Phys. Chem. B* **2005**, *109*, 12677.
- (5) Huang, J. X.; Kaner, R. B. *J. Am. Chem. Soc.* **2004**, *126*, 851.
- (6) Pool, R. *Science* **1990**, *247*, 1410.
- (7) Wan, M. X.; Huang, J.; Shen, Y. Q. *Synth. Met.* **1999**, *101*, 708.
- (8) Martin, C. R. *Science* **1994**, *266*, 1961.
- (9) Harada, M.; Adachi, M. *Adv. Mater.* **2000**, *12*, 839.
- (10) Dong, H.; Prasad, S.; Nyame, V.; Jones, W. E. *Chem. Mater.* **2004**, *16*, 371.
- (11) Wei, Z. X.; Wan, M. X.; Lin, T.; Dai, L. M. *Adv. Mater.* **2003**, *15*, 136.
- (12) Parthasarathy, R. V.; Martin, C. R. *Chem. Mater.* **1994**, *6*, 1627.
- (13) Qiu, H. J.; Wan, M. X.; Matthews, B.; Dai, L. M. *Macromolecules* **2001**, *34*, 675.
- (14) Wei, Z. X.; Wan, M. X. *Adv. Mater.* **2002**, *14*, 1314.
- (15) Sun, Z. C.; Geng, Y. H.; Li, J.; Jing, X. B.; Wang, F. S. *Synth. Met.* **1997**, *84*, 99.
- (16) Selvan, S. T.; Spatz, J. P.; Klok, H. A.; Moller, M. *Adv. Mater.* **1998**, *10*, 132.
- (17) Selvakannan, P. R.; Mandal, S.; Pasricha, R.; Adyanthaya, S. D.; Sastry, M. *Chem. Commun.* **2002**, *13*, 1334.
- (18) Liu, Y. C. *Langmuir* **2002**, *18*, 9516.
- (19) Kinyanjui, J. M.; Hatchett, D. W.; Smith, J. A.; Josowicz, M. *Chem. Mater.* **2004**, *16*, 3390.
- (20) Sarma, T. K.; Chattopadhyay, A. *Langmuir* **2004**, *20*, 4733.
- (21) Wang, Y.; Liu, Z. M.; Han, B. X.; Sun, Z. Y.; Huang, Y.; Yang, G. Y. *Langmuir* **2005**, *21*, 833.
- (22) Sarma, T. K.; Chattopadhyay, A. *J. Phys. Chem. A* **2004**, *108*, 7837.
- (23) Tian, S. J.; Liu, J. Y.; Zhu, T.; Knoll, W. *Chem. Mater.* **2004**, *16*, 4103.
- (24) Konyushenko, E. N.; Stejskal, J.; Sedenkova, I.; Trchova, M.; Sapurina, I.; Cieslar, M.; Prokes, J. *Polym. Int.* **2006**, *55*, 31.
- (25) Trchova, M.; Sedenkova, I.; Konyushenko, E. N.; Stejskal, J.; Holler, P.; Ciric-Marjanovic, G. *J. Phys. Chem. B* **2006**, *110*, 9461.
- (26) Stejskal, J.; Sapurina, I.; Trchova, M.; Konyushenko, E. N.; Holler, P. *Polymer* **2006**, *47*, 8253.

- (27) Chiou, N. R.; Lee, L. J.; Epstein, A. J. *Chem. Mater.* **2007**, *19*, 3589.
- (28) Hatchett, D. W.; Josowicz, M.; Janata, J. *J. Phys. Chem. B* **1999**, *103*, 10992.
- (29) Sun, Y. G.; Mayers, B.; Xia, Y. N. *Nano Lett.* **2003**, *3*, 675.
- (30) Kim, J. U.; Cha, S. H.; Shin, K.; Jho, J. Y.; Lee, J. C. *Adv. Mater.* **2004**, *16*, 459.
- (31) Shao, Y.; Jin, Y. D.; Dong, S. J. *Chem. Commun.* **2004**, *9*, 1104.
- (32) Panigrahi, G. P.; Sahu, B. P. *Int. J. Chem. Kinet.* **1991**, *23*, 989.
- (33) Hrapovic, S.; Liu, Y.; Enright, G.; Bensebaa, F.; Luong, J. H. T. *Langmuir* **2003**, *19*, 3958.
- (34) Rodriguez-Fernandez, J.; Perez-Juste, J.; Mulvaney, P.; Liz-Marzan, L. M. *J. Phys. Chem. B* **2005**, *109*, 14257.
- (35) Kan, C. X.; Zhu, X. G.; Wang, G. H. *J. Phys. Chem. B* **2006**, *110*, 4651.

CG060895C